

## Mixed Bloch-Néel-Ising character of 180° ferroelectric domain walls

Donghwa Lee (이동화),<sup>1</sup> Rakesh K. Behera,<sup>1</sup> Pingping Wu,<sup>2</sup> Haixuan Xu (徐海讚),<sup>1</sup> Y. L. Li,<sup>2</sup> Susan B. Sinnott,<sup>1</sup> Simon R. Phillpot,<sup>1</sup> L. Q. Chen,<sup>2</sup> and Venkatraman Gopalan<sup>2,\*</sup>

<sup>1</sup>Department of Materials Science and Engineering, University of Florida, Gainesville, Florida 32611, USA

<sup>2</sup>Department of Materials Science and Engineering, Pennsylvania State University, University Park, Pennsylvania 16802, USA

(Received 8 July 2009; published 12 August 2009; corrected 9 October 2009)

Ferroelectric 180° domain walls are well-known to be predominantly Ising-like. Using density functional theory, and molecular dynamics simulations, the 180° domain walls in prototypical ferroelectrics lead titanate (PbTiO<sub>3</sub>) and lithium niobate (LiNbO<sub>3</sub>) are shown to have mixed character; while predominantly Ising-like, they also manifest some Bloch- and Néel-like character. Phase-field calculations show that such mixed wall character can be dramatically enhanced in nanoscale thin film heterostructures such as BaTiO<sub>3</sub>/SrTiO<sub>3</sub>, where the internal wall structure can form polarization vortices. Such mixed character walls can be expected to exhibit dynamical wall properties distinct from pure Ising walls.

DOI: [10.1103/PhysRevB.80.060102](https://doi.org/10.1103/PhysRevB.80.060102)

PACS number(s): 77.80.Dj, 77.84.Dy, 68.65.Cd, 75.60.Ch

A ferroelectric material possesses a built-in electrical polarization that is switchable with an electric field; a ferromagnetic material possesses a built-in magnetization that is switchable with a magnetic field. A 180° magnetic wall is typically Bloch or Néel-type as shown schematically in Fig. 1. In switching by 180°, the magnetization vector either rotates in a plane parallel to the domain wall (Bloch) or normal to the domain wall (Néel). These rotations typically take place over many microns, a length scale that is a consequence of the ability of spins to overcome the weak spontaneous magnetostriction that couples lattice strain and magnetization. In contrast, spontaneous electrostriction, the coupling between ferroelectric polarization and lattice strain, imposes a significant energy cost for rotating the polarization away from the symmetry-allowed directions in the lattice. Thus a 180° ferroelectric wall is predominantly Ising-type. The resulting narrow, ideal 180° ferroelectric domain walls are thus generally understood to be fundamentally different from broad magnetic walls.

There are no exact equivalents of Bloch and Néel walls in single-phase ferroelectrics. This issue was considered long ago by Zhirnov<sup>1</sup> within the framework of phenomenological Ginzburg-Landau-Devonshire (GLD) theory. Subsequent works concluded that, based on material parameters, domain walls in ferroelectrics such as Rochelle salt<sup>2</sup> and BaTiO<sub>3</sub> (Ref. 3) should be predominantly Ising-like. Using GLD, Huang *et al.*<sup>4</sup> predicted the possibility of two mathematical solutions, one Ising-like and another Bloch-like polarization rotation in tetragonal BaTiO<sub>3</sub>. Padilla *et al.*<sup>5</sup> explored a 180° domain wall in tetragonal BaTiO<sub>3</sub> using Monte-Carlo simulation with an effective Hamiltonian, and confirmed their Ising-like nature along the tetragonal *z* axis. While they also found fluctuations in polarization in a direction orthogonal to the tetragonal polarization, they did not appear to be spatially correlated with the domain wall and were thus dismissed as computational artifacts. Meyer and Vanderbilt<sup>6</sup> predicted in-plane components at 90° walls in PbTiO<sub>3</sub>. Recently, vortex-type polarization distributions have been predicted in zero-dimensional ferroelectric nanodots.<sup>7,8</sup> When many crystallographically equivalent polarization directions are symmetry-allowed in ferroelastically distorted lattices, mini-

mization of the total energy of the system under free-surface elastic and electrical boundary conditions can result in multi-domain states with polarization vortices. By contrast, a single 180° Ising domain wall allows only two possible polarization directions across it, namely, up (+*P<sub>z</sub>*) and down (−*P<sub>z</sub>*). In this Rapid Communication, we show that additional polarization components, albeit small, do indeed exist at a 180°-domain wall in single-phase uniaxial ferroelectrics, leading to polarization rotations. In particular, we use a judicious combination of density functional theory (DFT) calculations, atomistic simulations with a classical potential, and GLD modeling to show that the polarization in ferroelectric domain walls can exhibit bulk-symmetry forbidden Bloch and Néel components in both PbTiO<sub>3</sub> and LiNbO<sub>3</sub>. Moreover, when the inherent stress energy at the interfaces in a multilayer heterostructure, such as BaTiO<sub>3</sub>/SrTiO<sub>3</sub>, overwhelms the bulk electrostrictive energy, the mixed wall character of these 180° domain walls becomes even more dramatic.

We first consider a (100) Pb-centered 180° wall in PbTiO<sub>3</sub>, a prototypical uniaxial perovskite ferroelectric with tetragonal 4mm symmetry, as shown in Fig. 2(a). Our DFT

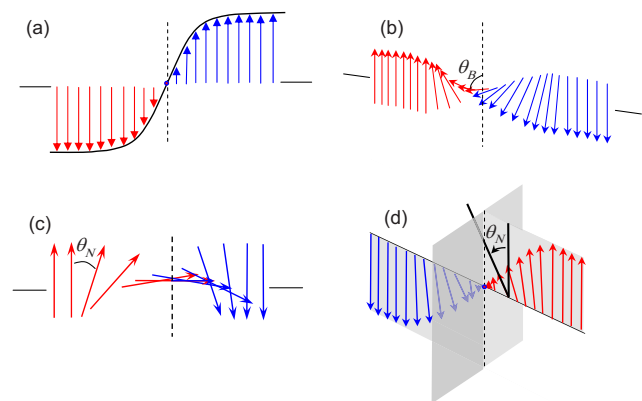


FIG. 1. (Color online) Different types of domain walls: (a) Ising type, (b) Bloch type, (c) Néel type, and (d) Mixed Ising-Néel type walls. A mixed Ising-Bloch type would look similar to (d) except that the rotation ( $\theta_B$ ) would be out of the plane of the polarization vector.

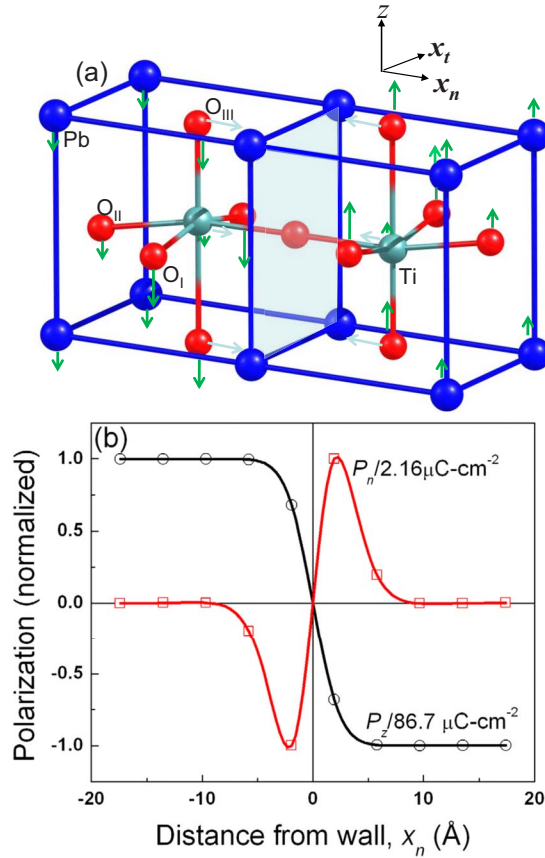


FIG. 2. (Color online) (a) The schematic of the atomic displacement across the domain wall along the normal direction is shown. The polarization was up ( $+P_z$ ) to the left and down ( $-P_z$ ) to the right of the domain wall. All the atoms move toward the domain wall for  $x_n$  displacements. For  $z$  displacements, all the atoms in the up domain displace along  $-z$  and in the down domain along  $+z$  direction with respect to their corresponding ferroelectric positions. The arrows for the  $z$ -displacement are scaled differently than the  $y$  displacements. The maximum  $z$  displacement was observed for  $O_I$  ( $\sim 0.07$  Å) and the minimum displacement was observed for Ti atoms ( $\sim 0.02$  Å). (b) Cell-by-cell normalized polarization ( $P_z$  and  $P_n$ ) as a function of the normal coordinate ( $x_n$ ) for (100)  $180^\circ$  Pb-centered domain wall. The open symbols are the polarization data points obtained from the final optimized structure and the solid lines are the fits to simulation results.

calculations use the Vienna *ab initio* software package. We used  $x \times 1 \times 1$  supercell ( $x=6, 8, 10 \dots 16$ ), where results converge for  $x \geq 10$ . Calculations have been performed with supercell dimensions fixed according to the corresponding single-crystal lattice parameters ( $a=3.8669$  Å,  $c/a=1.0436$ ), and allowing for expansion or contraction normal to the domain walls; the results are essentially identical in the two cases. In order to detect the presence of non-uniaxial components of polarization, the atoms are allowed to displace in all three spatial directions: parallel to the bulk polarization ( $z$  displacement), normal to the domain wall ( $x_n$  displacement) and parallel to the domain walls ( $x_t$  displacement). The cell-by-cell polarizations are calculated using the method of Meyer and Vanderbilt.<sup>6</sup> In agreement with previous calculations,<sup>6</sup> which determined the uniaxial polarization

$P_z$  through the domain wall, our DFT results show that Pb-centered walls are energetically favored over Ti-centered for (100)  $180^\circ$  domain walls. Also consistent with previous work, cell-by-cell polarization calculations show a 30% reduction in  $P_z$  from the bulk for unit cells around the Pb-centered domain wall. Analysis of the corresponding atomic displacements show that all the atoms move toward the domain wall. The oxygens on the Ti-centered plane [i.e.,  $O_{III}$  in Fig. 2(a)] relax the most ( $u_{n,O_{III}} \sim -0.03$  Å at  $x_n \sim 1.93$  Å) around the domain wall; the Ti atoms move by  $u_{n,Ti} \sim -0.01$  Å. All the other atoms show displacements of less than  $-0.005$  Å around the domain wall. In additional calculations, we manually removed the normal and parallel atom displacements, and then re-optimized the structure. In each case the atoms again displaced to the same positions, which suggests the robustness of these small non-uniaxial contributions to the polarization. The polarization component in the normal direction ( $P_n$ ) has a magnitude as high as  $P_{n,max} \sim 2.16$   $\mu\text{C}/\text{cm}^2$  out of the domain wall [Fig. 2(b)], which corresponds to  $\sim 2.5\%$  of the bulk polarization of  $86.7$   $\mu\text{C}/\text{cm}^2$ . There are no atom displacements along the transverse direction, and hence no polarization in the transverse ( $P_t$ ) direction parallel to the wall. The wall width is of the order of a unit cell for the  $P_z$  component. If we consider the vector sum  $\mathbf{P}_{total} = \mathbf{P}_z + \mathbf{P}_n + \mathbf{P}_t$ , we clearly see that  $P_n$  will lead to a Néel-like rotation of the polarization vector (by angle  $\tan \theta_N = P_n/P_z$ ) in the  $x_n$ - $z$  plane perpendicular to the domain wall. The maximum rotation angle,  $\theta_N$  [see Fig. 1(d)] for Pb-centered domain walls is  $\theta_N \sim 1.43^\circ$ , which indicates a mixed Ising-Néel-type domain wall in  $\text{PbTiO}_3$ . Calculations for (100) Ti-centered domain walls predicts a similar Ising-Néel-type wall character with  $P_n \sim 1.75\%$  of the bulk polarization value, and  $\theta_N \sim 1^\circ$ .

To demonstrate that Bloch-like domain walls are also possible, we next consider lithium niobate ( $\text{LiNbO}_3$ ), a classic uniaxial ferroelectric. Symmetry dictates that the ferroelectric polarization in a single domain state exist only along the  $c$ -axis (or  $z$ -axis),  $[0001]$ , that is  $P = \pm P_z$ . Using GLD, Scrymgeour *et al.* predicted non-Ising polarization components at  $180^\circ$  walls in  $\text{LiNbO}_3$ ,<sup>9</sup> which we now consider using DFT. We consider a wall along the crystallographic  $y$ - $z$  ( $\bar{1}\bar{1}20$ ) plane as shown in Fig. 3(a). Because of inherent computational constraints of DFT, we used a small  $4 \times 2 \times 1$  (240 atoms) simulation cell. Atomistic simulations on larger systems, with the interactions in  $\text{LiNbO}_3$  being described by an empirical interatomic potential,<sup>10</sup> yield qualitatively identical and quantitatively very similar polarization profiles. The DFT calculations provide good agreement with fundamental experimental (EXP) results for the single crystal, such as the polarization:  $70$   $\mu\text{C}/\text{cm}^2$  (EXP, 300 K) vs  $63.65$   $\mu\text{C}/\text{cm}^2$  (DFT, 0 K) and lattice parameters:  $a=5.148$  Å/ $c=13.863$  Å (EXP, 300 K) vs  $a=5.137$  Å/ $c=13.885$  Å (DFT, 0 K).

The lowest wall energy was found to be for a wall that lies halfway between the cation planes as shown in Fig. 3(a). DFT calculations yield wall energy of  $159$   $\text{mJ}/\text{m}^2$ . Figure 3(b) shows the various polarization components across the wall. Figures 3(c) and 3(d) depict the displacements of lithium and niobium near the wall in  $\text{LiNbO}_3$ , as determined

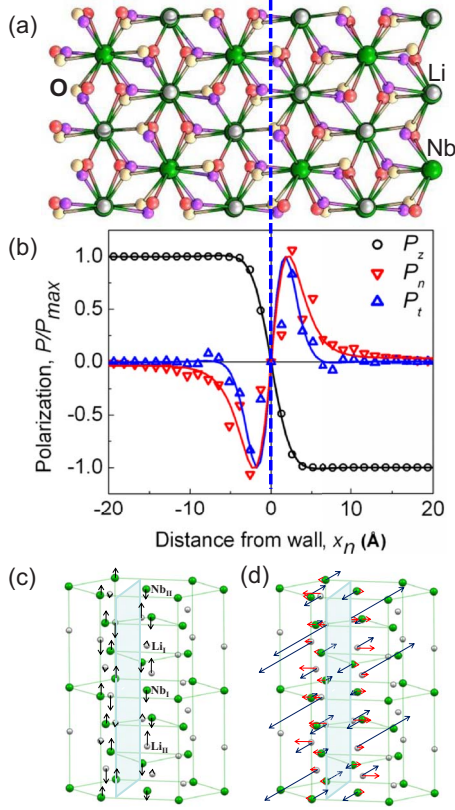


FIG. 3. (Color online) (a) Structural arrangement of LiNbO<sub>3</sub> near the lowest energy y-wall position projected in the (0001) plane; (b) the three polarization components,  $P_n$ ,  $P_t$ , and  $P_z$  as a function of the normal coordinate  $x_n$  across a single y-wall. The solid lines are fits to simulation results. (c) z-direction displacement of Li ( $u_{z, Li_I} = 0.001$  Å and  $u_{z, Li_{II}} = 0.023$  Å) and Nb ( $u_{z, Nb_I} = 0.019$  Å and  $u_{z, Nb_{II}} = 0.016$  Å) atoms in the near the y-wall; and (d) Wall normal ( $u_n$ ) and parallel ( $u_t$ ) displacements of Li ( $u_{n, Li_I} = 0.026$  Å,  $u_{n, Li_{II}} = 0.012$  Å,  $u_{t, Li_I} = 0.029$  Å, and  $u_{t, Li_{II}} = 0.088$  Å), and Nb atoms ( $u_{n, Nb_{II}} = 0.001$  Å,  $u_{n, Nb_I} = 0.014$  Å,  $u_{t, Nb_I} = 0.012$  Å, and  $u_{t, Nb_{II}} = 0.026$  Å) near a y-wall.

from atomistic simulations; again simulations for small systems show good agreement between the DFT and the atomistic calculations. The maximum polarization components are  $(P_n, P_t, P_z)_{max} = (0.56 \pm 0.001, 1.99 \pm 0.001, 62.4 \pm 0.01)$   $\mu\text{C}/\text{cm}^2$ . The presence of  $P_t$  thus leads to a Bloch-like rotation (by angle  $\tan \theta_B = P_t/P_z$ ) of the polarization vector in the  $x_t$ - $z$  plane of the domain wall in addition to the Néel-type rotation. The maximum rotation angles of  $\theta_B \sim 1.52^\circ$  and  $\theta_N \sim 0.55^\circ$  occur at a distance  $x_n \sim \pm 2.58$  Å from the wall where the  $P_t$  and  $P_n$  components are maximum, and the rotation disappears away from the wall, where  $P_t$  and  $P_n$  are zero. Thus, these walls have a mixed Ising-Bloch-Néel-type character.

Finally we show that such mixed wall character can be significantly enhanced in multilayer heterostructures of BaTiO<sub>3</sub>/SrTiO<sub>3</sub> in which the SrTiO<sub>3</sub> layers are under tensile strain, while the BaTiO<sub>3</sub> layers are under compressive strain. BaTiO<sub>3</sub> is a tetragonal ferroelectric (point group 4 mm) at room temperature, and its Curie temperature,  $T_c$  can be tuned over hundreds of degrees, significantly in thin film form, by the application of biaxial compressive or tensile strains.<sup>11</sup>

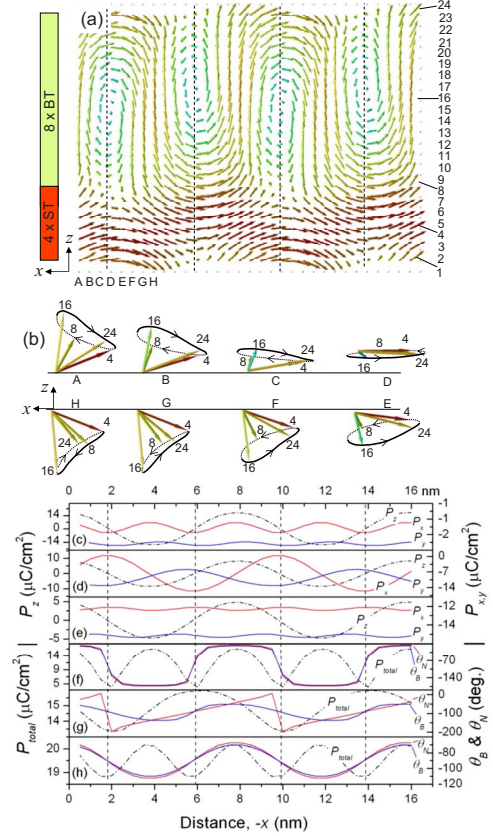


FIG. 4. (Color online) (a) Phase-field modeling of ferroelectric polarization vector distribution in a commensurate periodic (001) (SrTiO<sub>3</sub>)<sub>4</sub>/(001) (BaTiO<sub>3</sub>)<sub>8</sub> superlattice with four 180° domain walls indicated by vertical dashed lines, described in the text. The 24 rows are spaced every half a unit cell, and the 32 columns are spaced every 0.5 nm. (b) The polarization vector variation in the z direction for columns A-H across a single domain wall. The polarization components,  $P_x$  (or  $P_{x_n}$ ),  $P_y$  (or  $P_{y_t}$ ), and  $P_z$ , the total polarization,  $P_{total}$ , and the Bragg ( $\theta_B$ ) and Néel ( $\theta_N$ ) are shown as a function of coordinate  $x_n$  for the center of a SrTiO<sub>3</sub> layer (panels e, h) center of a BaTiO<sub>3</sub> layer (panels c, f), and the interface layer (panels d, g).

Similarly, SrTiO<sub>3</sub> is not ferroelectric in the bulk state, but can be driven into the ferroelectric state under biaxial strain.<sup>12</sup> Heterostructures of strained BaTiO<sub>3</sub>/SrTiO<sub>3</sub> have been explored experimentally,<sup>13</sup> using electronic-structure calculations<sup>14,15</sup> and with phase-field modeling.<sup>16</sup> Unusual polarization distributions across the interfaces<sup>14-16</sup> and property enhancements<sup>17,18</sup> have been reported. The polarization alternates between in-plane (SrTiO<sub>3</sub> layer) and out-of-plane (BaTiO<sub>3</sub> layer) directions alternately, which leads to polarization rotation across the interfaces, as has been shown by first principles<sup>14,15</sup> and phase-field calculations.<sup>16</sup> However, domain walls in such systems have been only minimally explored.<sup>19</sup> Here we use GLD calculations to demonstrate the mixed wall character of the polarization distribution across 180° domain walls in an example (BaTiO<sub>3</sub>)<sub>8</sub>/(SrTiO<sub>3</sub>)<sub>4</sub> heterostructure. The experimentally verified GLD free-energy potentials for BaTiO<sub>3</sub> and SrTiO<sub>3</sub> from Refs. 11 and 12 were used. Periodic boundary conditions were applied in the through-thickness direction and the

energy minimized without any substrate imposed strains (see Refs. 13 and 16 for modeling details). As a result BaTiO<sub>3</sub> layers are under  $-0.79\%$  compressive strain with  $T_c \sim 310$  K, and SrTiO<sub>3</sub> layers are under  $1.63\%$  tensile strain with  $T_c \sim 450$  K. Completely insulating films were assumed; dielectric losses can decrease depolarization charges at the interfaces and shift the  $T_c$ 's. At room temperature, under these strain conditions both BaTiO<sub>3</sub> and SrTiO<sub>3</sub> are thus ferroelectric. Figure 4(a) depicts the vector distribution of the total polarization,  $\mathbf{P}_{total}$ , across four  $180^\circ$  domain walls parallel to the  $y$ - $z$  plane. Interestingly, the internal structure of domain walls form polarization vortices with alternating handedness in traversing the wall normal,  $x$  (or  $x_n$ ). Figure 4(b) shows the variation of polarization in the  $z$  direction, where each vertical column of polarizations shows a complete  $360^\circ$  Bloch rotation about the  $z$  axis, as well as a Néel rotation on the order of  $\sim \pm 70^\circ$ . In the plane at the center of a BaTiO<sub>3</sub> layer [Figs. 4(c) and 4(f)] a  $180^\circ$  wall has a dominant Ising-like  $P_z$  component, but also possesses  $P_x$  and  $P_y$  with a maximum  $\theta_B \sim \theta_N \sim -172^\circ$  between pairs of domain walls. In the plane at the center of a SrTiO<sub>3</sub> layer [Figs. 4(e) and 4(h)] the non-Ising  $P_x$  and  $P_y$  components dominate, with maximum  $\theta_B \sim 110^\circ$  and  $\theta_N \sim 113^\circ$ . The interface plane [Figs. 4(d) and 4(g)] on the other hand is approximately equally mixed in character with  $\theta_B \sim 138^\circ$  and  $\theta_N \sim 196^\circ$ .

Thus these heterostructures exhibit mixed Ising-Bloch-Néel-type walls.

In conclusion, calculations from three complementary methods demonstrate that  $180^\circ$  ferroelectric domain walls in LiNbO<sub>3</sub> and PbTiO<sub>3</sub> that are known to be predominantly Ising-type, also possess components of Bloch- and Néel-like character. Since additional domain wall polarization components have been predicted in other ferroelectric systems as well, such as BaTiO<sub>3</sub> (Ref. 20) and BiFeO<sub>3</sub>,<sup>21</sup> such mixed wall character may be ubiquitous. The dynamics of such walls under external fields becomes extremely interesting and remains minimally explored.<sup>22,23</sup> The walls in BaTiO<sub>3</sub>/SrTiO<sub>3</sub> heterostructures appear to be broad (width  $\sim 3$ – $5$  nm or  $7$ – $12$  unit cells), and hence are expected to be ferroelectrically soft, considering the strong exponential dependence of the threshold field for wall motion on the width of the wall.<sup>24</sup> These observations should motivate further exploration of ferroelectric structures with non-Ising walls, and the resulting functionalities.

The authors would like to acknowledge funding from the National Science Foundation (Grants No. DMR-0820404, No. DMR-0507146, No. DMR-0908718, and No. DMR-0602986). We also thank the High Performance Computing (HPC), University of Florida for providing resources for the density functional theory calculations.

\*Corresponding author; vxg8@psu.edu

<sup>1</sup>V. A. Zhirnov, Zh. Eksp. Teor. Fiz. **35**, 1175 (1958).

<sup>2</sup>L. N. Bulaevskii, Fiz. Tverd. Tela (St. Petersburg) **5**, 3183 (1963).

<sup>3</sup>V. L. Ginzburg, Fiz. Tverd. Tela (St. Petersburg) **2**, 2031 (1960).

<sup>4</sup>X. R. Huang, X. B. Hu, S. S. Jiang, and D. Feng, Phys. Rev. B **55**, 5534 (1997).

<sup>5</sup>J. Padilla, W. Zhong, and D. Vanderbilt, Phys. Rev. B **53**, R5969 (1996).

<sup>6</sup>B. Meyer and D. Vanderbilt, Phys. Rev. B **65**, 104111 (2002).

<sup>7</sup>S. Prosandeev, I. Ponomareva, I. Naumov, I. Kornev, and L. Bellaiche, J. Phys.: Condens. Matter **20**, 193201 (2008).

<sup>8</sup>A. Gruverman, D. Wu, H.-J. Fan, I. Vrejoiu, M. Alexe, R. J. Harrison, and J. F. Scott, J. Phys.: Condens. Matter **20**, 342201 (2008).

<sup>9</sup>D. A. Scrymgeour, V. Gopalan, A. Itagi, A. Saxena, and P. J. Swart, Phys. Rev. B **71**, 184110 (2005).

<sup>10</sup>R. A. Jackson and M. E. G. Valerio, J. Phys.: Condens. Matter **17**, 837 (2005).

<sup>11</sup>K. J. Choi *et al.*, Science **306**, 1005 (2004).

<sup>12</sup>A. Vasudevarao *et al.*, Phys. Rev. Lett. **97**, 257602 (2006); also Y. L. Li, S. Choudhury, J. H. Haeni, M. D. Biegalski, A. Vasudevarao, A. Sharan, H. Z. Ma, J. Levy, V. Gopalan, S. Trolier-McKinstry, D. G. Schlom, Q. X. Jia, and L. Q. Chen, Phys. Rev. B **73**, 184112 (2006).

<sup>13</sup>D. A. Tenne *et al.*, Science **313**, 1614 (2006).

<sup>14</sup>K. Johnston, X. Huang, J. B. Neaton, and K. M. Rabe, Phys. Rev. B **71**, 100103(R) (2005).

<sup>15</sup>S. Lisenkov and L. Bellaiche, Phys. Rev. B **76**, 020102(R) (2007).

<sup>16</sup>Y. L. Li, S. Y. Hu, D. Tenne, A. Soukiassian, D. G. Schlom, L. Q. Chen, X. X. Xi, K. J. Choi, C. B. Eom, A. Saxena, T. Lookman, and Q. X. Jia, Appl. Phys. Lett. **91**, 252904 (2007).

<sup>17</sup>W. Tian, J. C. Jiang, X. Q. Pan, J. H. Haeni, Y. L. Li, L. Q. Chen, D. G. Schlom, J. B. Neaton, and K. M. Rabe, Appl. Phys. Lett. **89**, 092905 (2006).

<sup>18</sup>T. Zhao, Z. H. Chen, F. Chen, W. S. Shi, H. B. Lu, and G. Z. Yang, Phys. Rev. B **60**, 1697 (1999); A. Q. Jiang, J. F. Scott, Huibin Lu, and Zhenghao Chen, J. Appl. Phys. **93**, 1180 (2003).

<sup>19</sup>S. Lisenkov, I. Ponomareva, and L. Bellaiche, Phys. Rev. B **79**, 024101 (2009).

<sup>20</sup>V. Janovec, M. Grocký, V. Kopský, and Z. Kluiber, Ferroelectrics **303**, 65 (2004).

<sup>21</sup>J. Seidel *et al.*, Nature Mater. **8**, 229 (2009).

<sup>22</sup>Toru Shimuta, Osamu Nakagawara, Takahiro Makino, Seiichi Arai, Hitoshi Tabata, and Tomoji Kawai, J. Appl. Phys. **91**, 2290 (2002).

<sup>23</sup>M. Sepiarsky, S. R. Phillpot, D. Wolf, M. G. Stachiotti, and R. L. Migoni, Phys. Rev. B **64**, 060101(R) (2001).

<sup>24</sup>S. Choudhury *et al.*, J. Appl. Phys. **104**, 084107 (2008).